Competitive Binding of Protein Kinase Cα to Membranes and Rho GTPases†

Anthony C. Cook, Cojen Ho, Jennifer L. Kershner, Steve A. Malinowski, Heath Moldveen, Brigid A. Stagliano, and Simon J. Slater*

Department of Pathology and Cell Biology, Thomas Jefferson University, Philadelphia, Pennsylvania 19107

Received June 22, 2006; Revised Manuscript Received October 2, 2006

ABSTRACT: Previously, we have shown that protein kinase Cα (PKCα) forms a direct high-affinity, isozyme-specific and membrane lipid-independent interaction with Rho GTPases [Slater, S. J., Seiz, J. L., Stagliano, B. A., and Stubbs, C. D. (2001) *Biochemistry 40*, 4437−4445]. Since the cellular activation of PKCα involves an initial translocation from cytosolic to membrane compartments, the present study investigates the interdependence between the direct protein−protein interaction of PKCα with the Rho GTPase, Cdc42, and the protein−lipid interactions of PKCα with membranes. It was hypothesized that the interaction of PKCα with membrane-bound Cdc42 would contribute to the overall membrane-binding affinity of the kinase by providing an additional anchor. However, it was found that the incorporation of isoprenylated Cdc42 into membranes resulted in an apparent *decrease* in the membrane-binding affinity of PKCα, whereas the association of PKC*β*I, PKC*δ*, PKC*ϵ*, and PKC*ζ* was each unaffected. The presence of membrane-bound Cdc42 resulted in a rightward shift in both the PS- and Ca^{2+}-concentration response curves for PKCα membrane association and for the ensuing activation, whereas the maximal levels of binding and activation attained at saturating PS and Ca^{2+} concentrations were in each case unaffected. Overall, these findings suggest that PKCα undergoes a isozyme-specific interaction with membrane-bound Cdc42 to form a PKCα−Cdc42 complex, which possesses a membrane-binding affinity that is *reduced* relative to that of the individual components due to competition between Cdc42 and PS/Ca^{2+} for binding to PKCα. Consistent with this, it was found that the interaction of PKCα with membrane-bound Cdc42 was accompanied by the physical dissociation of the PKCα−Cdc42 complex from membranes. Thus, the study provides a novel mechanism by which the membrane association and activation of PKCα and Cdc42 may be regulated by competing protein−protein and protein−lipid interactions.

Protein kinase C (PKC)[1] consists of a family of minimally 12 serine−threonine kinases that occupy critical nodes in receptor-initiated signaling networks which regulate both normal and pathological cellular processes, including secretion, proliferation, differentiation, apoptosis, and migration (*1*−*8*). Each of the isozymes can be classified into three groups based upon the presence or absence of structurally conserved domains that dictate activator dependences for membrane association and activation (*5*, *7*, *9*). In the case of the "conventional" PKCα, -*β*I/*β*II, and -*γ* isozymes, these include the activator-binding C1 domains and the Ca^{2+}-binding C2 domain. The C1 domains consist of a tandem C1A and C1B arrangement, each of which can potentially bind the endogenous activator, diacylglycerol, and exogenous activators including phorbol esters (*10*, *11*). The "novel" PKC*δ*, -*ϵ*, -*η*, -*θ*, and -*μ* isozymes contain C2 domains that lack Ca^{2+}-binding ability, while retaining functional C1A and C1B domains. The "atypical" PKC*ζ*, -*ι*, and -*λ* regulatory domains also lack a functional C2 domain and contain a single C1 domain that lacks the ability to bind activators, the function of which remains obscure. Each isozyme becomes catalytically competent by undergoing multiple serine−threonine and tyrosine phosphorylations that are either autocatalytic or catalyzed by another upstream kinase, such as the phosphoinositide-dependent kinase, PDK1 (*6*).

The cellular activation of PKC isozymes is accompanied by a reversible translocation from cytosol to membrane compartments that is elicited by receptor- and phospholipase C-coupled DAG production and inositol trisphosphate-mediated Ca^{2+} release from internal stores (*5*). The initial interaction of the conventional PKC isozymes with the membrane is mediated by the formation of a relatively low affinity Ca^{2+} bridge between anionic residues in the C2 domain and the head group of phosphatidylserine (PS), which then facilitates the interaction of either DAG with the C1A domain or the tumor-promoting phorbol esters with the C1B domain (*5*, *11*, *12*). These parallel but independent protein−lipid interactions supply the activation energy for a conformational change in the membrane-associated PKC molecule

† This work was supported by U.S. Public Health Service Grants AA010990 and AA010968.

* To whom correspondence should be addressed. Tel: (215) 503-5019. Fax: (215) 923-2218. E-mail: Simon.Slater@jefferson.edu.

[1] Abbreviations: DOGS-NTA/Ni^{2+}, 1,2-dioleoyl-*sn*-glycero-3-{[*N*-(5-amino-1-carboxypentyl)iminodiacetic acid]succinyl} nickel salt; EYPC, chicken egg L-α-phosphatidylcholine; FC, flow cell; FRET, fluorescence resonance energy transfer; GMP-PNP, guanosine 5′-[*β*,*γ*-imido]triphosphate trisodium salt; HAF, 5-hexadecanoylaminofluorescein; HSC-T6, immortalized hepatic stellate cell line−T6; LUV, large unilamellar vesicles; MBP_{4-14}, bovine myelin basic protein peptide substrate; MANT-GMP-PNP, 3′-*O*-(*N*-methylanthraniloyl)-*β*,*γ*-imidoguanosine 5′-triphosphate trisodium salt; PKCα, α-isoform of protein kinase C; POPS, 1-palmitoyl-2-oleoyl-*sn*-glycero-3-phosphoserine; RhoGDIα, α-isoform of Rho GDP-dissociation inhibitor; SPR, surface plasmon resonance.

10.1021/bi0612420 CCC: $33.50 © 2006 American Chemical Society
Published on Web 11/09/2006

that leads to the displacement of an autoinhibitory pseudosubstrate from the active site, allowing substrate binding and phosphorylation to occur (*13*−*15*).

The low molecular weight Rho GTPases that belong to the Ras superfamily each play a central role in many cellular processes, including the regulation of actin cytoskeleton dynamics, gene transcription, cell cycle progression, and membrane trafficking (*16*, *17*). The closely related mammalian Rho GTPase family consists of minimally 14 members, of which RhoA, Cdc42, and Rac1 have been widely studied with respect to their roles in the regulation of the cytoskeleton (*18*, *19*), and their structures and molecular mechanisms of action have been characterized in detail (*16*, *20*). Similar to the PKC isozymes, the Rho GTPases also act as tightly regulated molecular switches by cycling between inactive GDP-bound cytosolic forms and active GTP-bound membrane-associated forms. Each of the Rho GTPases are retained in an inactive GDP-bound state in the cytosol by interaction with the Rho GDP-dissociation inhibitor (RhoGDI), and translocation to the membrane is triggered by a guanine nucleotide exchange factor (GEF) catalyzed GDP exchange for GTP (*16*, *21*). Membrane association is also coupled to posttranslational modifications which consist of the sequential attachment of a geranylgeranyl chain to a cysteine residue within a conserved C-terminal CAAX domain, followed by proteolysis of the three C-terminal residues and carboxymethylation (*20*). In general, the GTP-bound membrane-associated form of each Rho GTPase can then specifically interact with and activate membrane-associated downstream targets or effectors, examples of which include phospholipases D (*22*−*24*) and C (*25*, *26*), rhophillin (*27*), diacylglycerol kinase *θ* (*28*),several protein kinases including PKN (*27*, *29*), PRK1, and 2 (*30*, *31*), and the Rho-associated kinases p160-ROCK and p150-ROK-α and -*β* (*32*, *33*).

Recent studies have provided evidence supporting cross-talk between PKC and Rho GTPase mediated signaling pathways and have revealed a close association between the mammalian proteins (*34*−*41*) and also between the yeast homologues Pkc1p and Rho1p (*42*, *43*). In particular, studies from this laboratory have shown that PKCα undergoes a direct, isozyme-specific and lipid-independent protein−protein interaction with RhoA, Cdc42, and to a lesser extent Rac1 (*44*, *45*). In each case this interaction was shown to result in kinase activation with respect to the phosphorylation of a downstream PKCα substrate, supporting the notion that PKCα should be added to the list of downstream effectors for these Rho GTPases. Both the interaction and the ensuing PKCα activation were found to be dependent on the Ca^{2+}- and DAG/phorbol ester-induced conformational state of PKCα and also on the GTP/GDP-induced conformational states of the Rho GTPases. Whereas it was necessary to exclude membrane lipids from the assay systems used in the previous study in order to provide evidence for a direct protein−protein interaction between PKCα and Rho GTPases (*44*), the conformational changes in each protein that result in activation both occur at the membrane. Thus, an important question remains whether there is interdependence between the direct protein−protein interaction of PKCα with Rho GTPases and the protein−lipid interactions that mediate the membrane association of the kinase.

The aim of this study was to investigate the interplay between protein−lipid and protein−protein interactions in the association of PKCα with membranes containing the Rho GTPase, Cdc42. It was initially hypothesized that if the direct PKCα−Cdc42 interaction occurred at the membrane surface, then this would result in an enhancement of PKCα membrane association by providing an additional anchoring element in addition to Ca^{2+}/PS binding to the C2 domain and DAG/phorbol ester binding to the C1 domains. However, it was found that the incorporation of Cdc42 into membranes resulted in a *decrease* in the membrane-binding affinity of PKCα, which was observed as a rightward shift in the PS- and Ca^{2+}-concentration dependencies for both membrane association and activation. Thus, whereas the results indicate that the previously reported direct interaction between PKCα and Cdc42 also occurs at the membrane surface, the findings suggest that the binding affinity of the resultant PKCα−Cdc42 complex is *reduced* relative to each of the individual protein components. Consistent with this, the PKCα−Cdc42 complex formed by the direct interaction between the two proteins at the membrane surface was found to physically dissociate from the membrane. These findings provide a novel mechanism by which the interaction of PKCα and Cdc42 with downstream targets could be regulated by competing protein−protein and protein−lipid interactions.

MATERIALS AND METHODS

Materials. Primers, Grace's insect media, phosphate-buffered saline (PBS), 5-hexadecanoylaminofluorescein (HAF), 3′-*O*-(*N*-methylanthraniloyl)-*β*,*γ*-imidoguanosine 5′-triphosphate trisodium salt (MANT-GMP-PNP), and *Spodoptera frugiperda* (Sf9) cells were each obtained from Invitrogen Technologies (Carlsbad, CA), and the hepatic stellate cell line−T6 (HSC-T6) was a kind gift from Dr. William S. Blaner (Department of Medicine, Columbia University, New York). The L1 sensor chip was purchased for use in a Biacore 2000 SPR system from Biacore, Inc. (Piscataway, NJ). Fetal bovine serum (FBS), protease inhibitor cocktail, guanosine 5′-[*β*,*γ*-imido]triphosphate trisodium salt (GMP-PNP), and all other research grade chemicals were from Sigma (St. Louis, MO). Chicken egg L-α-phosphatidylcholine (EYPC), 1-palmitoyl-2-oleoylphosphatidylserine (POPS), and 1,2-dioleoyl-*sn*-glycero-3-{[*N*-(5-amino-1-carboxypentyl)iminodiacetic acid]succinyl} nickel salt) (DOGS-NTA/Ni^{2+}) were from Avanti Polar Lipids, Inc. (Alabaster, AL). Adenosine 5′-triphosphate (ATP) was from Boehringer Mannheim (Indianapolis, IN), and [*γ*-^{32}P]ATP was from New England Nuclear (Boston, MA). Baculovirus encoding human Cdc42 N-terminal tagged with 6×His was a kind gift from Dr. R. A. Cerione (Department of Molecular Medicine, Veterinary Medical Center, Cornell University, New York), and a baculovirus containing RhoGDI N-terminal tagged with GST was custom manufactured by Orbigen (San Diego, CA). Where required, free Ca^{2+} and Mg^{2+} concentrations in EDTA buffers were calculated using the program "MAXC" at http://www.stanford.edu/~cpatton/maxc.html (*46*), which takes into account the total concentrations of EDTA, Ca^{2+}, and Mg^{2+} present in the assay system.

Baculovirus Construction. Recombinant PKCα, PKC*β*I, PKC*δ*, PKC*ϵ*, and PKCζ (rat brain) were each prepared using the Bac-to-Bac baculovirus Sf9 cell expression system (Invitrogen, Carlsbad, CA) as originally described (*47*), with

modifications (*48*), and purified to homogeneity by following published procedures (*48*, *49*). The isoforms PKCδ, PKCϵ, and PKCζ were overexpressed in Sf9 cells as fusion proteins containing a 6×His attached to the C-terminus (*48*) and were purified as described previously (*48*, *50*). Baculovirus containing human RhoA N-terminal tagged with 6×His was also prepared using the Bac-to-Bac baculovirus SF9 cell expression system (Invitrogen, Carlsbad, CA). Briefly, the RhoA coding sequence was double digested from pUSEamp-RhoA (Upstate, Lake Placid, NY) using *Eco*RI/*Xho*I and ligated into the baculovirus transfer vector pfastbacHta. Correct ligation was confirmed by colony PCR, and the construct was recombined with bacmid according to the manufacturer's instructions (Invitrogen, Carlsbad, CA). Expression of proteins was confirmed by SDS−PAGE followed by Western blotting using the ECL system (Amersham Biosciences, Piscataway, NJ) and the appropriate primary antibodies (Cytoskeleton, Inc., Ann Arbor, MI).

*Coexpression of RhoA and Cdc42 with RhoGDI*α. Since the presence of the geranylgeranyl chain attached to the C-terminus of RhoA and Cdc42 reduces their aqueous solubility, each protein was coexpressed and purified as a complex with RhoGDIα-GST, as described previously (*51*). In this complex, the geranylgeranyl chain of each Rho GTPase is shielded from the aqueous environment by insertion into a hydrophobic binding pocket on RhoGDIα (*52*, *53*). Briefly, log phase Sf9 cells in 1 L of Grace's insect media containing 10% FBS were infected with baculovirus encoding Cdc42-6×His or RhoA-6×His and RhoGDIα-GST at a multiplicity of infection of 5, 1, and 2, respectively, followed by incubation for 4 days. The cells were then washed once with PBS, pelleted, and then lysed using a Dounce homogenizer in buffer A (50 mM Tris-HCl, pH 8.0, 150 mM NaCl, 5 mM $MgCl_2$) containing a protease inhibitor cocktail. The cell debris was removed by centrifugation at 3500*g* for 15 min (4 °C), and the resultant supernatant was centrifuged at 100000*g* for 1 h to pellet membranes. The supernatant was incubated with Ni^{2+}/NTA chelating resin in buffer A for 45 min at 4 °C with gentle rocking, and the resin was then packed into a 5 mL column attached to an ÄKTApurifier FPLC system (GE Healthcare, Piscataway, NJ). The column was washed with buffer A until the absorbance of the flow-through at 280 nm was <0.01 absorbance unit. The bound protein was then eluted from the column by incubation with buffer A containing 50 mM imidazole. Fractions containing the required proteins were pooled and incubated with glutathione resin in buffer A for 60 min at 4 °C with gentle rocking. Following this, the resin was again packed into a 5 mL column, which was washed with buffer A until the flow-through had an absorbance at 280 nm of <0.01 absorbance unit. The bound protein was then eluted with buffer A containing 15 mM reduced glutathione, and the pooled eluted protein was dialyzed against buffer B (10 mM HEPES, 150 mM NaCl, 5 mM $MgCl_2$) for 36 h with buffer changes every 12 h. Protein concentration was determined by the Bradford protein assay (Bio-Rad, Faraday, CA), and protein was stored at −80 °C in buffer B containing 20% glycerol. The stoichiometry of the Cdc42−RhoGDIα complex was determined to be 1:1 using Coomassie Blue staining (results not shown).

Preparation of HSC-T6 Plasma Membranes. The HSC-T6 cell line was chosen as a source of plasma membranes due to the established presence of both PKC- and Rho GTPase-mediated signaling in these cells and also due to the high growth rate (see, e.g., ref *54* and a review in ref *55*). Cells were grown to confluency in 10 mL of Waymouth's MB 752/1 media (Gibco) supplemented with 10% (v/v) fetal bovine serum (Sigma) and 1% (v/v) penicillin/streptomycin (Gibco) under a 5% CO_2 atmosphere at 37 °C. The media were then removed, and the cells were harvested by scraping in 10 mL of PBS followed by low-speed centrifugation. Each of the proceeding steps was performed at 4 °C. Pellets were resuspended in a lysis buffer consisting of 10 mM HEPES, pH 7.5, and 20 mM imidazole with 1% protein inhibitor cocktail (Sigma) by passage through a 20-gauge needle five times, followed by passage through a 23-gauge needle ten times. Lysates were then pooled, briefly sonicated, centrifuged at 1500*g* for 15 min, and then made up to ∼35 mL in lysis buffer in a 50 mL centrifuge tube. The suspension was then centrifuged at 1000*g* for 12 min, and the resultant supernatant was centrifuged at 8000*g* for a further 20 min. The resultant supernatant was again transferred to a clean tube and centrifuged at 100000*g* for 30 min. The pellet was then homogenized in lysis buffer and applied to a 35%−45% sucrose gradient. After centrifugation at 50000*g* for 120 min, the plasma membrane fraction present at the interface between the 35% and 45% layers was removed and suspended in 20 mM Tris-HCl (pH 7.4). The plasma membranes were pelleted by centrifugation at 100000*g* for 30 min, resuspended in 20 mM Tris-HCl (pH 7.4), and stored at −80 °C.

Preparation of Vesicles. Large unilamellar vesicles (LUV) were prepared from lipids as described previously (*49*). Briefly, chloroform solutions of EYPC, POPS, and DAG (500 μM total lipid concentration) were mixed in a test tube, and the solvent was removed under a stream of nitrogen to form a homogeneous thin film. The required volume of buffer (10 mM HEPES, pH 7.4, 150 mM NaCl) was then added, and the lipids were allowed to hydrate for 15 min at 25 °C. Following this, multilamellar vesicles were formed by vortexing for 1 min. Large unilamellar vesicles of 100 nm diameter (LUV) were prepared from multilamellar vesicles by the extrusion technique, using an Avestin Liposofast extruder (MM Developments, Ottawa, Canada), also as previously described (*56*). The mole fractions of EYPC, POPS, and DAG in the LUV were $(100 - X)$:X:4, respectively, where X is the required mole fraction of POPS.

Surface Plasmon Resonance (SPR) Determinations. The membrane association of RhoA, Cdc42, and PKCα was quantified from the time dependence of the accompanying increase in the SPR signal (response) using a Biacore 2000 (Biacore, Inc., Piscataway, NJ). All measurements were performed at 25 °C using a running buffer consisting of 10 mM HEPES, pH 7.4, and 150 mM NaCl. Briefly, the hydrophobic surface of an L1 sensor chip was initially cleaned by two injections of 10 mM CHAPS, and EYPC/POPS/DAG LUV of the required composition was then captured on this surface at a flow rate of 5 μL/min and a contact time of 15 min. Previous studies have shown that the L1 chip surface is completely covered under the conditions used and that the resultant lipid surface resembles a rough bilayer structure (*57*, *58*). For experiments involving HSC-T6 plasma membranes, lipid concentrations were estimated on the basis of a protein:lipid mass ratio of 1:4.

Each membrane surface was then conditioned with sequential injections of 10 mM glycine (pH 1.5) and 10 mM NaOH in order to remove loosely associated vesicles and to minimize baseline drift. The RhoA−RhoGDIα or Cdc42−RhoGDIα complex was diluted to the required final concentration in buffer B containing 50 μM GMP-PNP, and the free Mg^{2+} concentration was reduced to <0.5 μM by chelation with 14.3 mM EDTA in order to trigger nucleotide exchange and initiate complex dissociation. The final complex concentration present in experiments was typically 0.5 M, unless otherwise stated. The resultant mixture was then immediately injected over the EYPC/POPS/DAG surface at a flow rate of 10 μL/min, and binding due to capture of geranylgeranylated Rho GTPases was monitored as a function of time. For determinations of the effects of Cdc42 on PKC isozyme binding to membranes, Cdc42 was in each case captured to a level of ~200 response units, unless otherwise stated. Since binding response is directly proportional to the mass of Cdc42 bound to the membrane surface, the surface concentration of Cdc42 was identical in each experiment. After equilibration for 5 min, the required PKC isozyme, each diluted to a final concentration of 10 nM in a buffer containing 10 mM HEPES (pH 7.4), 150 mM NaCl, and 0.1 mM Ca^{2+}, was injected over the surface at a flow rate of 20 μL/min, and the increase in response resulting from PKC binding was measured as a function of time. Following each co-injection, the chip surface was regenerated with three 10 μL injections of CHAPS at a flow rate of 5 μL/min.

Analysis of SPR Data. Whereas the Biacore system allows affinity constants to be determined from the ratio of association and dissociation rate constants, the rates of dissociation of Cdc42 and PKCα from membranes were in each case found to be too slow for accurate determination of a dissociation rate constant. The binding constants for the interaction of PKCα and Cdc42 with membranes were therefore determined by measuring the extent of PKCα ($R_{eq,PKC\alpha}$) or Cdc42 binding at equilibrium ($R_{eq,Cdc42}$) as a function of the concentration of PKCα or the Cdc42−RhoGDIα complex injected. For the determination of binding constants from POPS- and Ca^{2+}-concentration dependences for the membrane association of PKCα, values of $R_{eq,PKC\alpha}$ for PKC binding were measured as a function of POPS mole fraction or free Ca^{2+} concentration. Values of $R_{eq,PKC\alpha}$ were obtained by fitting the response (R_t) verses time curves for each analyte concentration to an integrated first-order rate equation using nonlinear regression analysis:

$$R_t - R_{eq,PKC\alpha} = (R_0 - R_{eq,PKC\alpha})[1 - \exp(-k_{obs}t)] \quad (1)$$

where R_0 is the initial response and k_{obs} is the observed first-order rate constant. Values of $R_{eq,PKC\alpha}$ as a function of analyte concentration data were then fitted to a modified Hill equation (*59*):

$$R_{eq,PKC\alpha} = R_0 + R_{max}[C^n/(K_{app}{}^n + C^n)] \quad (2)$$

where R_0 is the initial response in the absence of analyte, R_{max} is the response corresponding to maximal occupation of membrane binding sites, C is the concentration of analyte, K_{app} is the apparent association constant, and n is the Hill coefficient. Goodness of fit was assessed from values of the average squared residual (χ^2).

Detection of the Dissociation of the PKCα−Cdc42 Complex from Membranes by SPR. In order to determine whether the PKCα−Cdc42 complex dissociates from membranes, advantage was taken of the ability to link the flow cells of the Biacore 2000 system in series, so that the output of the first flow cell (FC) was directed over the surface of the second (Figure 5A). Briefly, membranes composed of EYPC and DAG (96:4, molar), EYPC, POPS, and DAG (76:20:4, molar), or HSC-T6 plasma membranes were captured on the surface of FC1, and Cdc42 was then incorporated into these membrane surfaces by inducing the dissociation of the Cdc42−RhoGDIα complex (0.5 M) upon Mg^{2+} chelation, as described above. Membranes composed of EYPC and DOGS-NTA/Ni^{2+} at a molar ratio of 95:5 were captured on the surface of FC2. The output of FC1 was then directed to the input of FC2, and PKCα (10 nM) in a buffer containing 10 mM HEPES (pH 7.4), 150 mM NaCl, and 0.1 mM Ca^{2+} was injected into FC1 at a flow rate of 20 μL/min. The Ni^{2+} chelating lipid, DOGS-NTA/Ni^{2+}, binds 6×His-tagged proteins with high affinity (*60*). On the basis of this, the dissociation of the Cdc42−PKCα complex from membranes in FC1 was determined from a corresponding increase in response in FC2 resulting from the specific binding of the complex to DOGS-NTA/Ni^{2+} through the 6×His-tagged Cdc42.

Fluorescence-Based Assay of Cdc42−PKCα and Cdc42−RhoGDI Complex Dissociation from Membranes. The dissociation of the Cdc42−PKCα and Cdc42−RhoGDIα complex from membranes was determined from the accompanying decrease in fluorescence energy transfer (FRET) between the MANT fluorophore of MANT-GMP-PNP bound to Cdc42 and the membrane probe, HAF, based on a previously described method (*61*, *62*). For these experiments, Cdc42 was expressed in Sf9 cells and purified in the absence of RhoGDIα using procedures that were identical to that described above for the Cdc42−RhoGDIα complex, except that the purification by glutathione affinity chromatography was omitted. Cdc42 was initially loaded with MANT-GMP-PNP as described previously (*62*). Briefly, to 60 nM Cdc42 in buffer B containing 2 μM MANT-GMP-PNP was added 14.3 mM EDTA, which triggers nucleotide exchange by reducing the free Mg^{2+} concentration to <0.5 μM. The emission fluorescence intensity of MANT-GMP-PNP was then measured at 25 °C as a function of time at 430 nm upon excitation at 355 nm using an ISS modified LSM 48000 multifrequency phase and modulation fluorometer. Upon attaining a stable baseline, LUV composed of either EYPC/DAG (96:4, molar) or EYPC/POPS/DAG (76:20:4, molar) containing 2 M HAF (300 μM total lipid concentration) were added and allowed to equilibrate for 30 min. To this, either PKCα at the required concentration or 60 nM RhoGDIα in buffer B was added, and the emission fluorescence intensity of MANT-GMP-PNP was measured as a function of time.

Measurement of Cdc42-Induced PKCα Activity in the Presence of Membranes. PKCα activity was assayed by measuring the rate of phosphate incorporation into a peptide corresponding to the phosphorylation site domain of myelin basic protein (QKRPSQRSKYL, MBP_{4-14}). The assay (75 μL) consisted of 50 mM Tris-HCl (pH 7.4), 0.1 mM $CaCl_2$, 50 μM MBP_{4-14}, and LUV composed of EYPC, DAG, and POPS (150 μM) in the molar ratio (100 − X):4:X, where X is the required mole fraction of POPS. Cdc42 was captured

on LUV by dissociation of the Cdc42−RhoGDIα complex (100 nM), triggered by nucleotide exchange and Mg^{2+} chelation in buffer B containing 50 μM GMP-PNP with 14.3 mM EDTA. For lipid-free assays, free Cdc42 purified in the absence of RhoGDIα was added at a concentration of 100 nM. After thermal equilibration to 30 °C, assays were initiated by the simultaneous addition of PKCα (0.1 nM) along with 15 mM Mg^{2+}, 15 μM ATP, and 0.3 μCi of [γ-^{32}P]-ATP (3000 Ci/mmol) and terminated after 30 min with 100 μL of 175 mM phosphoric acid. Following this, 100 μL was transferred to P81 filter papers, which were washed three times in 75 mM phosphoric acid. The phosphorylated peptide was quantified by scintillation counting.

RESULTS

On the basis of our previous observation that PKCα forms a direct protein−protein interaction with RhoA, Cdc42, and to a lesser extent Rac1 (*44*), it was hypothesized that such an interaction occurring at the membrane would result in an enhanced level of PKCα membrane association. In order to address this, the effect of the presence of recombinant Cdc42 incorporated into membranes of defined lipid composition on the association of purified recombinant PKCα with these membranes was determined along with the corresponding effects on kinase activity.

Incorporation of Cdc42 into Membranes. In order to determine the effects of membrane-bound Cdc42 on PKCα membrane association, geranylgeranylated Cdc42 was initially captured on membranes composed of EYPC and DAG (96:4, molar), which were immobilized on the hydrophobic surface of a Biacore L1 sensor chip (*57*, *58*). This was achieved by inducing the dissociation of the corresponding RhoGDIα complex by triggering GDP-−GMP-PNP exchange on Cdc42 upon Mg^{2+} chelation (*61*, *63*). It was found that the injection of the Cdc42−RhoGDIα complex in the presence of GMP-PNP and excess EDTA resulted in a time-dependent increase in binding to EYPC/DAG membranes (Figure 1A). The extent of Cdc42 binding at equilibrium was found to be markedly reduced when either EDTA or GMP-PNP was absent and to be negligible in the absence of both compounds. This indicates that the Cdc42−RhoGDIα complex has a negligible affinity for the membranes used and that the observed binding signal resulted from the membrane association of Cdc42.

The binding constants for the interaction of Cdc42 with membranes were determined from fits of $R_{eq,Cdc42}$ against the concentration of the Cdc42−RhoGDIα complex to eq 2 (Figure 1B, ●). Values of $R_{eq,Cdc42}$ were obtained from fits of the association phases of Cdc42 binding as a function of time data obtained with increasing concentrations of the Cdc42−RhoGDIα complex to eq 1, which are shown for illustration in Figure 1C. The value of K_{app} for the interaction of Cdc42 with EYPC/DAG/POPS membranes was 0.5 ± 0.2 μM, which is ∼15-fold greater than the value determined in a previous study of the affinity constant for the interaction of GMP-PNP-loaded Cdc42 with RhoGDI in the absence of membranes (28 nM) (*61*). This indicates that the release of Cdc42 from the RhoGDI complex is likely to correspond to the rate-determining step in the association of the Rho GTPase with membranes under the experimental conditions used in the present study. The value of the Hill coefficient

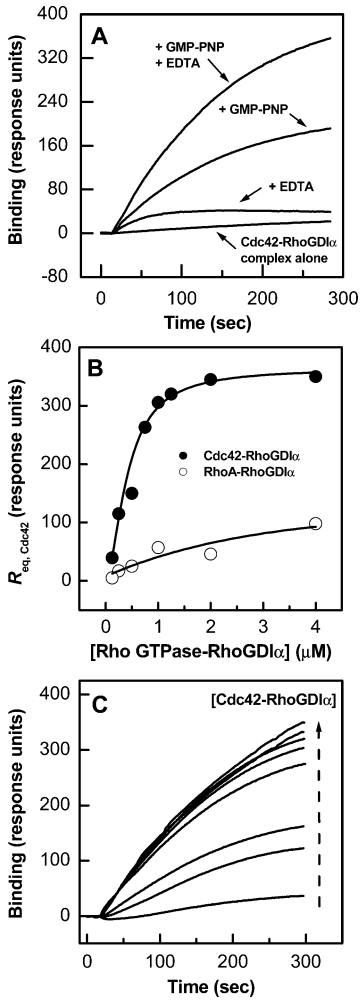

FIGURE 1: Membrane association of Cdc42 triggered by the dissociation of the RhoGDIα−Cdc42 complex. (A) Time-dependent increase in Cdc42 binding to EYPC/DAG/POPS membranes due to dissociation of the RhoGDIα−Cdc42 complex in the presence of 50 μM GMP-PNP and 14.3 mM EDTA (free Mg^{2+} > 0.5 μM), separately or combination, and in the absence of GMP-PNP and EDTA. (B) Binding of Cdc42 and RhoA to EYPC/DAG/POPS membranes at equilibrium ($R_{eq,Cdc42}$) as a function of the Cdc42−RhoGDIα or RhoA−RhoGDIα complex concentration. Values of $R_{eq,Cdc42}$ were obtained from fits of the association phases of Cdc42 binding as a function of time data measured for increasing concentrations of the RhoGDIα−Cdc42 complex shown in panel C to eq 1. The data are representative of triplicate experiments. Other details are given under Materials and Methods.

(*n*) for the interaction of Cdc42 with EYPC/DAG membranes resulting from dissociation from the RhoGDIα complex was 1.1 ± 0.2, indicating a lack of cooperativity with respect to Cdc42−RhoGDIα complex dissociation and Cdc42 membrane association. By contrast to Cdc42, the injection of the RhoA−RhoGDIα complex under the same conditions used for dissociation of the Cdc42−RhoGDIα complex resulted in only a marginal level of RhoA binding to membranes (Figure 1B, ○). Due to this, the effects of membrane-bound RhoA on PKCα membrane association were not addressed in the present study.

The possibility that RhoGDIα may also associate with membranes upon dissociation of the complex and thus might contribute to the observed binding signal was ruled out in separate control experiments which showed that purified RhoGDIα alone bound negligibly to membranes within a

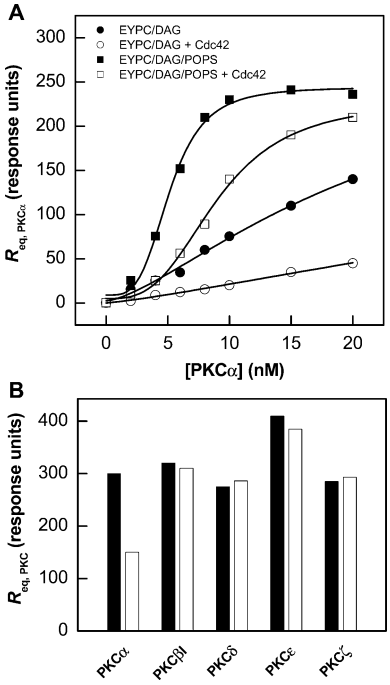

FIGURE 2: Effect of membrane-bound Cdc42 on the membrane association of PKCα. (A) The interaction of PKCα with EYPC/DAG (●, ○) and EYPC/DAG/POPS (■, □) membranes ($R_{eq,PKC\alpha}$) was determined in the presence of 0.1 mM Ca^{2+} either with (○, □) or without Cdc42 (●, ■). Solid curves correspond to fits of each data set to eq 2. (B) Values of $R_{eq,PKC}$ obtained for the interaction of PKCα, PKC*β*I, PKC*δ*, PKC*ε*, and PKCζ, each at a level of 10 nM, with EYPC/POPS/DAG membranes in the presence (open bars) and absence (solid bars) of Cdc42. In each case Cdc42 was initially captured on the membrane by dissociation from the RhoGDIα−Cdc42 complex to a level of ∼200 Ru. Data are each representative of three independent experiments. Other details are described in Materials and Methods.

concentration range that would be present assuming complete dissociation of the Cdc42−RhoGDIα complex (results not shown).

*Effects of Membrane-Bound Cdc42 on the Membrane Association of PKC*α. The effect of membrane-bound Cdc42 on the membrane association of PKCα was investigated by injecting increasing levels of the isozyme in the presence of Ca^{2+} over an EYPC/DAG (96:4, molar) or EYPC/DAG/POPS (76:4:20, molar) surface, with or without membrane-incorporated Cdc42 (Figure 2). In order to avoid the possibility that the presence of Cdc42 on membranes might limit the availability of lipid binding sites for PKCα, the level of Cdc42 captured on membranes in FC1 in these experiments was ∼200 Ru, which is submaximal with respect to Cdc42 binding (see Figure 1B). Also, the mole fraction of DAG (4 mol %) and Ca^{2+} concentration (0.1 mM) used have been shown previously to be sufficient for the optimal membrane association and activation of PKCα (*64*−*66*).

In the absence of Cdc42, PKCα was found to bind with relatively low affinity to EYPC/DAG membranes, and the affinity of this interaction was enhanced by the presence of 20 mol % POPS in these membranes, as expected (Figure 2, closed symbols). The value of $K_{app} = 5.2 \pm 0.2$ nM determined from data obtained in the presence of POPS is close to that reported in a recent SPR-based study of the interaction of PKCα with membranes of similar composition (*67*). PKCα binding to EYPC/DAG/POPS membranes was found to be cooperative with respect to the PKCα injection concentration ($n = 3.0 \pm 0.1$), which is in keeping with the results of recent reports suggesting that this isozyme may self-associate at the membrane surface (*68*−*70*). The presence of Cdc42 on EYPC/DAG or EYPC/DAG/POPS membranes was in each case found to result in a marked decrease in the extent of PKCα binding (Figure 2, open symbols). On the basis of the data obtained for EYPC/DAG/POPS membranes, this effect appeared to correspond to a rightward shift in the concentration−response curve, as reflected by an increase in the value of K_{app} to 9.4 ± 0.4 nM. The presence of Cdc42 and POPS also resulted in a decrease in the value of n to 2.1 ± 0.2 relative to that obtained without Cdc42, suggesting that the presence of the Rho GTPase at the membrane surface decreases the cooperativity of the PKCα−membrane interaction.

Since we have previously shown that the direct interaction between PKCα and Cdc42 that occurs in the absence of membranes is a specific property of this isozyme (*44*), the question arises whether the inhibitory effects of Cdc42 on membrane association may also share similar isozyme specificity. In order to address this, the effects of a fixed level of Cdc42 captured on EYPC/POPS/DAG membranes on the association of equimolar concentrations of PKCα, PKC*β*I, PKC*δ*, PKC*ε*, and PKC were determined (Figure 2B). It was found that only the association of PKCα with membranes was significantly inhibited by the presence of membrane-bound Cdc42, consistent with an isozyme-specific interaction between PKCα and Cdc42 at the membrane surface.

*Effects of Cdc42 on the PS and Ca^{2+} Dependence of PKC*α *Membrane Association.* The effects of membrane-bound Cdc42 on PKCα membrane association were determined as a function of the mole fraction of POPS in EYPC/DAG membranes at a fixed level of Ca^{2+} (0.1 mM) and also as a function free Ca^{2+} levels at a fixed mole fraction of POPS (20 mol %). Values of $R_{eq,PKC\alpha}$ were determined from fits of PKCα binding as a function of time data obtained for each POPS mole fraction and free Ca^{2+} concentration in the presence and absence of membrane-associated Cdc42 to eq 1 using nonlinear regression analysis (results not shown). Plotting values of $R_{eq,PKC\alpha}$ obtained in the absence of Cdc42 against the POPS mole fraction (Figure 3A, ●) yielded a sigmoidal concentration response curve, which is consistent with the results of previous studies (*64*, *65*), as was the Ca^{2+} concentration−response for the interaction of PKCα with EYPC/DAG/POPS membranes of composition 76:4:20, molar (Figure 3B, ●) (*59*, *71*). The values of K_{app} and n obtained from fits of these curves to eq 2 (Table 1), were also found to be in close agreement with previously reported values (*59*, *64*, *65*, *71*). Also consistent with previous results (*59*), a relatively small amount of PKCα binding was observed in the presence of 4 mol % DAG and 20 mol % POPS with Ca^{2+} absent (Figure 3A) and also with 4 mol % DAG and 0.1 mM Ca^{2+} with POPS absent (Figure 3B).

The level of PKCα binding to EYPC/DAG membranes was found to be unaffected by the presence of Cdc42 at saturating mole fractions of POPS (Figure 3A, ○) or Ca^{2+} (Figure 3B, ○), whereas PKCα binding at submaximal levels was in each case decreased. Furthermore, the values of K_{app} obtained from fits of $R_{eq,PKC\alpha}$ versus POPS mole fraction or free Ca^{2+} concentration were both increased in the presence of Cdc42 by ∼2- and ∼5-fold, respectively (Table 1), which

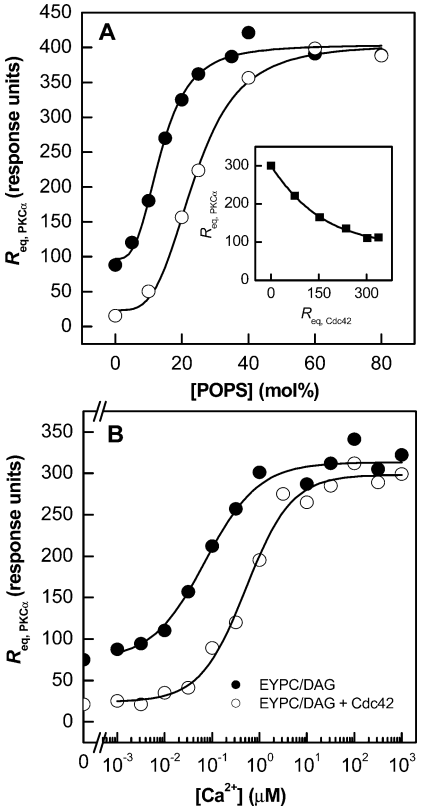

FIGURE 3: Effect of membrane-bound Cdc42 on the POPS- and Ca^{2+}-concentration dependences for PKCα membrane association. (A) Values of $R_{eq,PKC\alpha}$ for PKCα binding to membranes composed of EYPC/DAG/POPS in the molar ratio (100 − *X*):*X*:4, where *X* is the mole fraction of POPS, were determined in the presence of 0.1 mM Ca^{2+}, with (○) or without Cdc42 (●) initially captured on the membrane by dissociation from the RhoGDIα−Cdc42 complex to a level of 200 Ru, from fits of the association phases of the corresponding response verses time curves to eq 1. Inset: Dependence of $R_{eq,PKC\alpha}$ binding to EYPC/POPS/DAG membranes (76:20:4, molar) on the amount of Cdc42 captured ($R_{eq,Cdc42}$). (B) Values of $R_{eq,PKC\alpha}$ for PKCα binding to EYPC/DAG/POPS membranes (76:4:20, molar) were determined as a function of free Ca^{2+} concentration, with (○) or without Cdc42 (●) initially captured on the membrane by dissociation from the RhoGDIα−Cdc42 complex to a level of ∼200 Ru, from fits of the association phases of the corresponding response verses time curves to eq 1. Solid curves correspond to fits of each data set to eq 2. Data represent the means of triplicate determinations from two independent experiments. Other details are described in Materials and Methods.

reflected a rightward shift in both of the concentration−response curves. However, values of *n* obtained from POPS- and Ca^{2+}-concentration responses were in each case unaffected by the presence of Cdc42 (Table 1). The Cdc42-concentration dependence of the inhibitory effect on the association of PKC with membranes composed of EYPC/POPS/DAG (76:20:4, molar) was determined by plotting values of $R_{eq,PKC\alpha}$ as a function of the amount of Cdc42 captured, $R_{eq,Cdc42}$ (Figure 3A, inset). It was found that the extent of PKCα binding to membranes decreased as a function of the concentration of membrane-bound Cdc42 in a saturable manner, suggesting a specific interaction between PKCα and Cdc42 at the membrane surface.

Effects of Cdc42 on the PS and Ca^{2+} Dependence of Membrane-Associated PKCα Activation. The results presented so far indicate that the presence of Cdc42 at the surface of EYPC/DAG membranes leads to a decrease in the membrane-binding affinity of PKCα and suggest that this effect may involve competition between Cdc42 and PS/Ca^{2+} for interaction with the isozyme. In order to address whether the apparent decrease in membrane-binding affinity translates into an effect on membrane-associated PKCα activity, the effects of Cdc42 on the PS- and Ca^{2+}-concentration dependences for activation induced by association with EYPC/DAG membranes were determined (Figure 4). In the absence of Cdc42, it was found that the POPS concentration−response curve for PKCα activation with EYPC/DAG LUV and 0.1 mM Ca^{2+} coincided with that obtained for membrane association (compare Figures 4A and 3A, ●), as shown by the similar values of K_{app} and *n* derived from fits of the activity data to eq 2 (Table 1). This finding is consistent with the results of previous studies showing that the PS dependences of PKC activation and membrane association are linearly related (*64*, *72*). Comparison of the Ca^{2+} response curve for PKCα activation (Figure 4B, ●) with that obtained for binding to EYPC/DAG membranes (Figure 3B, ●) indicates that the Ca^{2+} levels required to induce PKC activity are ∼2 orders of magnitude greater than those required for membrane association, which is again consistent with previous findings (*59*, *71*). The low level of PKCα binding to EYPC/DAG membranes that was observed in the absence of either POPS (Figure 3A) or Ca^{2+} (Figure 3B) did not appear to result in a measurable increase in the level of activity under the same conditions (Figure 4), suggesting that under these conditions PKCα is associated with membranes in an inactive state.

The presence of membrane-associated Cdc42 was found have biphasic effects on the POPS- and Ca^{2+}-concentration−response curves for PKCα activation (Figure 4, ○). Thus, similar to the effects on PKCα binding to EYPC/DAG membranes (Figure 3), each curve was found to be shifted to the right, which was again reflected by an increase in the corresponding values of K_{app} by ∼2- and 5-fold, respectively (Table 1). Furthermore, the values of *n* obtained from these curves were found to be unaffected by the presence of Cdc42, as was the case for PKCα binding to EYPC/DAG membranes (Table 1). However, contrasting with effects on membrane association, the level of activity obtained within low POPS and Ca^{2+} concentration ranges was found to be increased in the presence of Cdc42 (Figure 4, ○). Notably, the level of PKCα activity determined in the absence of POPS was found to be close to that induced by the direct interaction of the enzyme with Cdc42 measured in the absence of membranes (Figure 4A, inset).

Table 1: Effects of Membrane-Bound Cdc42 on the PS- and Ca^{2+}-Concentration Responses for Membrane Association and Activation of PKCα[a]

	POPS		Ca^{2+}	
	K_{app} (mol %)	*n*	K_{app} (μM)	*n*
membrane association	12 ± 1	3.0 ± 0.5	0.09 ± 0.01	1.0 ± 0.1
	24 ± 1[b]	3.0 ± 0.5[b]	0.50 ± 0.09[b]	0.9 ± 0.1[b]
activation	11 ± 1	3.0 ± 0.3	11 ± 1.6	1.0 ± 0.1
	21 ± 2[b]	3.0 ± 0.5[b]	60 ± 3.5[b]	1.0 ± 0.2[b]

[a] Values of affinity constants (K_{app}) and Hill coefficients (*n*) were obtained from fits of R_{eq} versus POPS mole fraction or free Ca^{2+} concentration data shown in Figures 3 and 4, respectively, to a modified Hill equation (*59*). [b]Values of K_{app} and *n* obtained in the presence of membrane-bound Cdc42. Errors in values are ± standard deviation. See Materials and Methods for details.

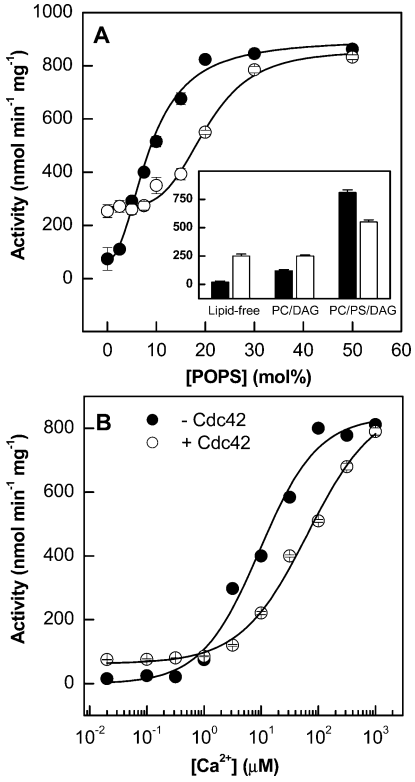

FIGURE 4: Effect of membrane-bound Cdc42 on POPS- and Ca^{2+}-concentration dependences for PKCα activation. (A) The activity of PKCα was measured in the presence of 0.1 mM Ca^{2+} and LUV composed of EYPC/DAG/POPS in the molar ratio (100 − *X*):*X*:4, where *X* is the mole fraction of POPS in the presence (○) and absence (●) of Cdc42 bound to membranes upon dissociation of the RhoGDIα−Cdc42 complex (0.5 μM). Inset: The effects of Cdc42 on membrane-associated and lipid-free activities and PKCα activity were determined in the presence of Ca^{2+} (0.1 mM) and EYPC/DAG (96:4, molar) or EYPC/DAG/POPS (76:4:20, molar) or in the absence of LUV, with (open bars) and without Cdc42 (solid bars). For lipid-free assays, free Cdc42 purified in the absence of RhoGDIα was added at a concentration of 100 nM. (B) The activity of PKCα was measured in the presence of EYPC/DAG/POPS membranes (76:4:20, molar) as a function of free Ca^{2+} concentration, with (○) or without Cdc42 (●) captured on the membrane by dissociation from the RhoGDIα−Cdc42 complex (0.5 μM). Solid curves correspond to fits of each data set to eq 2. Data represent the means of triplicate determinations from three independent experiments. Other details are described in Materials and Methods.

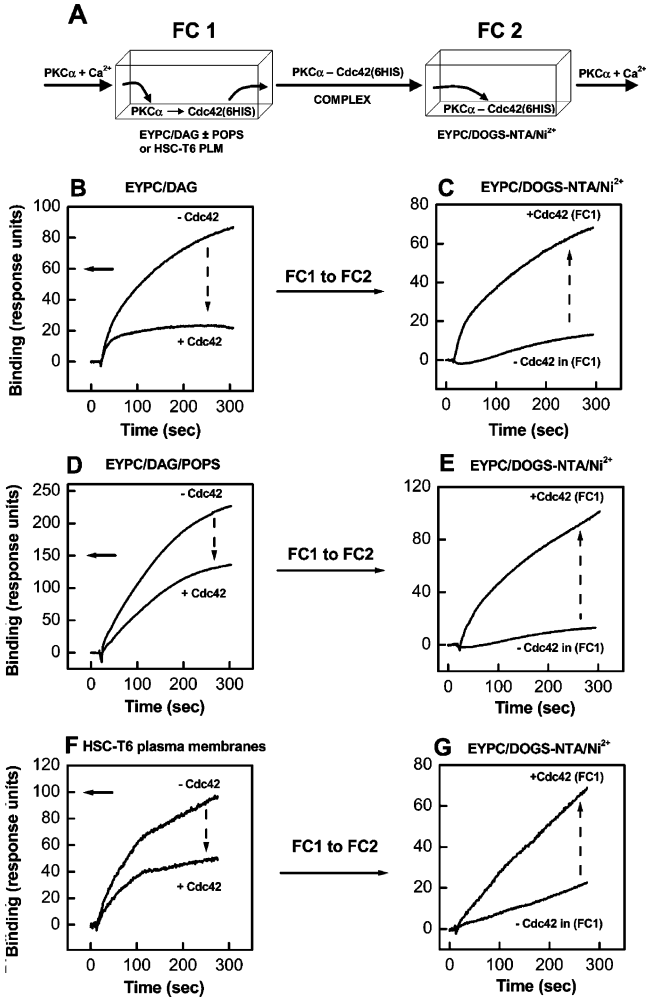

FIGURE 5: Dissociation of the PKCα−Cdc42 complex from membranes detected from SPR measurements. In the experimental system used (panel A), FC1 and FC2 of a Biacore L1 chip were connected in series. PKCα was injected (10 nM) in the presence of 0.1 mM Ca^{2+} over EYPC/DAG (96:4, molar) membranes (panel B), EYPC/DAG/POPS (76:4:20, molar) membranes (panel D), or HSC-T6 plasma membranes (panel F) immobilized in FC1 with or without Cdc42 initially captured by dissociation from the RhoGDIα−Cdc42 complex to the levels indicated (solid arrows). Binding of the PKCα−Cdc42 complex to EYPC/DOGS-NTA/Ni^{2+} (95:5, molar) membranes in FC2 was determined upon injection of PKCα over each membrane in FC1 with or without Cdc42 (panels C, E, and G). Data are representative of experiments carried out in triplicate. Other details are described in Materials and Methods.

Detection of the Membrane Dissociation of the PKCα−Cdc42 Complex by Measurements of SPR. The apparent reduction in the binding affinity of PKCα for EYPC/DAG membranes that results from interaction with membrane-bound Cdc42 raises the intriguing possibility that the PKCα−Cdc42 complex thus formed may physically dissociate from the membrane. This possibility was investigated by linking the output of the first flow cell of the L1 chip (FC1) to the input of the second flow cell (FC2), as illustrated in Figure 5A. The second membrane surface immobilized in FC2 was composed of EYPC and the Ni^{2+} chelating lipid, DOGS-NTA/Ni^{2+} (95:5, molar), which binds 6×His-tagged proteins with high affinity (*60*). Thus, separate control experiments confirmed that this DOGS-NTA/Ni^{2+}surface bound 6×His-tagged Cdc42 in a specific manner, whereas the extent of PKCα binding to this surface was marginal at the concentration present in experiments (results not shown). This arrangement therefore allowed the PKCα−Cdc42 complex dissociating from the membrane surface in FC1 to be detected as an increase in response in FC2 due to its specific capture on the DOGS-NTA/Ni^{2+}surface through the 6×His-tagged Cdc42.

The level of PKCα binding at equilibrium to EYPC/DAG membranes incorporating Cdc42 captured in FC1 was found to be reduced by ∼75% compared to that obtained in the absence of Cdc42 (Figure 5B), which is consistent with the data shown in Figure 2. Importantly, the injection of PKCα over the EYPC/DAG surface with Cdc42 present in FC1 resulted in a time-dependent increase in the level of binding to the DOGS-NTA/Ni^{2+}surface in FC2, the magnitude of which was similar to the amount by which PKCα binding in FC1 was decreased (Figure 5C). This is in keeping with the capture of the PKCα−Cdc42 complex on the DOGS-NTA/Ni^{2+}surface in FC2 due to its dissociation from the EYPC/DAG surface in FC1. Since the amount of Cdc42

initially captured on the EYPC/DAG surface in FC1 was ~60 Ru, and the increase in binding in FC2 due to PKCα−Cdc42 complex capture was ~60 Ru, then the percentage of Cdc42 extracted from the EYPC/DAG membrane in FC1 by injection of 10 nM PKCα over this surface was ~[60-(M_w of Cdc42/M_w of PKCα)/60] × 100 ~ 25%.

The extent of binding of PKCα to EYPC/POPS/DAG membranes (76:4:20, molar) captured in FC1 was again found to be reduced in the presence of Cdc42 (Figure 5D), and this again corresponded to an increase in the level of binding to the DOGS-NTA/Ni^{2+}surface in FC2 (Figure 5E). Moreover, the amount by which binding observed in FC2 was increased due to the presence of Cdc42 on POPS-containing membranes in FC1 was similar to the amount by which PKCα binding to these membranes was decreased. However, the magnitude of these effects of Cdc42 (~30%) was reduced compared to that observed in the absence of POPS (Figure 5B). The amount of Cdc42 initially captured on the EYPC/POPS/DAG surface in FC1 was ~150 Ru, and the increase in binding in FC2 due to complex capture was ~85 Ru. Therefore, the percentage of Cdc42 extracted from the EYPC/POPS/DAG membrane in FC1 by injection of 10 nM PKCα over this surface was ~[85(M_w of Cdc42/M_w of PKCα)/150] × 100 ~ 15%.

In order to address the question whether PKCα may also extract Cdc42 from plasma membranes, PKCα was injected with Ca^{2+} over HSC-T6 plasma membranes immobilized on FC1 in the presence and absence of Cdc42 (Figure 5F). Similar to effects on PKCα binding to LUV, the extent of PKC binding to HSC-T6 plasma membranes in FC1 was again found to be reduced in the presence of membrane-bound Cdc42 (~100 Ru), and this reduction in binding again corresponded to a similar increase in binding to the DOGS-NTA/Ni^{2+} surface in FC2 (Figure 5G). The percentage of Cdc42 extracted from the plasma membranes was ~[55(M_w of Cdc42/M_w of PKCα)/100] × 100 ~ 15%.

Membrane Dissociation of the PKCα−Cdc42 Complex Detected by Measurements of FRET. In order to provide further evidence supporting the physical dissociation of the PKCα−Cdc42 complex from membranes, the ability of PKCα to extract membrane-bound Cdc42 was determined on the basis of measurements of FRET between the MANT-donor fluorophore of MANT-GMP-PNP loaded onto Cdc42 and the membrane-associated acceptor fluorophore of HAF. This experimental paradigm has been used previously for studies of the kinetic properties of the extraction of Cdc42 from membranes by RhoGDI (*61*, *62*). Thus, in order to validate observations made with PKCα, initial experiments were undertaken to confirm that Cdc42 could be extracted from the EYPC/DAG/POPS membranes by RhoGDIα under the experimental conditions used in the present study. It was found that the addition of EYPC/DAG/POPS (76:4:20, molar) labeled with 2 M HAF quenched the emission fluorescence intensity of MANT-GMP-PNP loaded on Cdc42 by ~50%, which is consistent with FRET between MANT and HAF fluorophores at the membrane surface (Figure 6A). The addition of RhoGDIα at an equimolar concentration with Cdc42 (60 nM) was found to result in a rapid dequenching of MANT emission fluorescence due to a decrease in FRET, which was promoted slightly by the addition of excess Mg^{2+} (Figure 6A). These observations are in keeping with those reported previously (*61*, *62*) and confirm that MANT-GMP-PNP-loaded Cdc42 is extracted from membranes by RhoGDIα under the present experimental conditions.

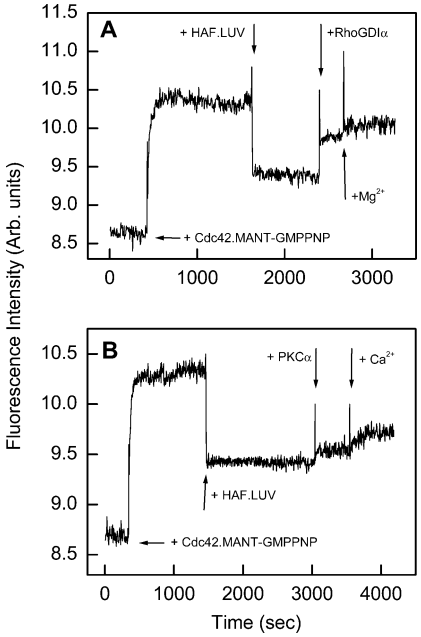

FIGURE 6: Dissociation of the PKCα−Cdc42 complex from membranes detected on the basis of FRET. The emission fluorescence intensity at 430 nm upon excitation at 355 nm was measured as function of time, with sequential additions of MANT-GMP-PNP (2 μM) loaded on Cdc42 (60 nM) and LUV composed EYPC/POPS/DAG (76:20:4, molar) containing 2 μM HAF (300 μM total lipid concentration). (A) Recovery of fluorescence quenching upon addition of 60 nM RhoGDIα followed by Mg^{2+} (1 mM free concentration). (B) Fluorescence recovery resulting from the addition of PKCα (65 nM) followed by Ca^{2+} (0.1 mM free concentration). Data are representative of experiments carried out in duplicate. Other details are described in Materials and Methods.

Similar to RhoGDIα, the addition of PKCα to EYPC/POPS/DAG/HAF LUV incorporating MANT-GMP-PNP-loaded Cdc42 again resulted in a dequenching of MANT emission fluorescence (Figure 6B), which is consistent with the physical dissociation of the PKCα−Cdc42 complex from the membrane. The MANT-fluorescence dequenching due to extraction of Cdc42 was further promoted by the addition of excess Ca^{2+} whereas neither the rate nor the magnitude of extraction from membranes was found to be affected upon replacement of Ca^{2+} with an excess of Mg^{2+} (results not shown). It was also found in a separate control experiment that the addition of Ca^{2+} alone in the absence of PKCα did not affect the emission fluorescence intensity of MANT (results not shown).

The concentration-dependent effects of PKCα on the kinetics of the extraction of Cdc42 from EYPC/DAG and EYPC/POPS/DAG LUV were determined on the basis of plots of the percentage extraction of Cdc42 against time (Figure 7). The maximal levels of Cdc42 extraction from EYPC/DAG and EYPC/POPS/DAG LUV were in each case found to increase with PKCα concentration (Figure 7) and to attain saturation (Figure 7A, inset). Whereas the rate of PKCα-mediated extraction from EYPC/DAG LUV was found to be decreased compared to that induced by RhoGDIα, the extent of Cdc42 extraction from these LUV induced by saturating levels of PKCα approached that observed with RhoGDIα (Figure 7A). Furthermore, consistent with the SPR results shown in Figure 5, the extent of extraction was found

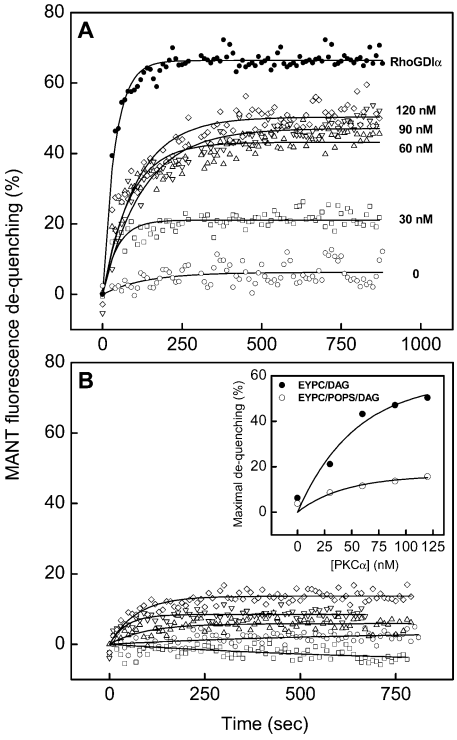

FIGURE 7: PKCα concentration dependence of the extraction of Cdc42 from membranes. The percentage extraction of Cdc42 induced by the addition of increasing levels of PKCα together with a fixed level of 0.1 mM Ca^{2+} was determined as a function of time for LUV composed of 96:4, molar, EYPC/DAG (panel A) or 76:20:4, molar, EYPC/POPS/DAG (panel B). The PKCα concentrations used were 0 (○), 30 (□), 60 (△), 90 (▽), and 120 (◇). For comparison, the time course for the fluorescence dequenching by the addition of RhoGDIα and 1 mM Mg^{2+} (●) is shown in panel A. Percentage extraction was calculated from (MANT fluorescence increase due to extraction at time = *t*)/(MANT fluorescence decrease due to MANT quenching by HAF) × 100. Solid curves correspond to fits of each data set to a first-order rate equation. Inset: Maximal percentage extraction of Cdc42 from EYPC/DAG (●) and EYPC/POPS/DAG (○) LUV plotted as a function of PKCα concentration. Data are representative of experiments carried out in duplicate. Other details are described in Materials and Methods.

to be markedly reduced by the incorporation of 20% POPS in these LUV (Figure 7B).

DISCUSSION

In this study, the interplay between the direct protein−protein interaction of PKCα with Cdc42 and the protein−lipid interactions that mediate the membrane association of this isozyme was investigated. It was found that the isozyme-specific protein−protein interaction previously shown to occur between Cdc42 and PKCα in the absence of lipids (*44*, *45*) is also retained at the membrane surface. Whereas it was initially hypothesized that this protein−protein interaction would supplement the PS- and Ca^{2+}-mediated protein−lipid interactions that anchor PKCα at the membrane, it was found that the interaction of PKCα with Cdc42 *competed* with the interaction of PKCα with PS and Ca^{2+}, resulting in a net *decrease* in membrane-binding affinity. In order to investigate the effects of membrane-bound Cdc42 on the membrane association of PKCα, a novel procedure was developed for immobilizing geranylgeranylated Cdc42 on membranes captured on the surface of a Biacore L1 sensor chip by inducing the dissociation of the Cdc42−RhoGDIα complex. Using this approach, it was found that the observed decrease in membrane-binding affinity corresponded to the physical dissociation of the PKCα−Cdc42 complex from membranes composed of purified lipids and also from isolated HSC-T6 plasma membranes. The results point to a novel mechanism for the regulation of the association of PKCα and Cdc42 with membranes by competing protein−protein and protein−lipid interactions (Figure 8).

Membrane Association of Cdc42 Is Triggered by the Dissociation of the RhoGDIα Complex. The steps that lead to the functional activation of Rho GTPases include the release from the corresponding cytosolic RhoGDI complex, membrane association of the Rho GTPase, and GEF-catalyzed exchange of GDP for GTP (*16*, *21*). However, the order of these events and the mechanism by which the membrane cycling of Rho GTPases and nucleotide exchange are coupled remain unclear. Thus, it has been suggested that GEFs interact with and catalyze nucleotide exchange on the cytosolic Rho GTPase−RhoGDI complex, which then promotes the dissociation of the complex and the translocation of the Rho GTPases to membranes (*73*, *74*). Alternatively, the dissociation of the RhoGDI−Rho GTPase complex and the translocation of GDP-bound Rho GTPases to membranes might precede GEF-catalyzed GDP-GTP exchange (*75*). The present observation that binding to membranes upon injection of the Cdc42−RhoGDIα complex was only detected in the presence of EDTA and GMP-PNP (see Figure 1A) indicates that nucleotide exchange on Cdc42 bound to RhoGDIα is both necessary and sufficient for Cdc42 membrane association and that this can occur even in the absence of a GEF. Consistent with this, it was shown recently that the association of Rac1 with asolectin liposomes was induced by triggering the dissociation of the Rac1−RhoGDI complex upon Mg^{2+} chelation and nucleotide exchange and that this was facilitated by the GEF, Tiam1 (*63*).

The observation that GDP-GMP-PNP exchange triggers the dissociation of the Cdc42−RhoGDIα complex and the membrane association of Cdc42 indicates that GMP-PNP-bound Cdc42 either has a lower binding affinity for RhoGDIα or has a higher affinity for EYPC/DAG/POPS membranes compared to GDP-bound Cdc42. Interestingly, it has been reported previously that, in the absence of membranes, RhoGDIα binds to both the GDP- and GTP-bound forms with equivalent affinities (*61*). Thus, the present results suggest that GMP-PNP-bound Cdc42 may have a higher affinity for EYPC/DAG/POPS membranes compared to the corresponding GDP-bound form, and further experiments are currently underway in the laboratory to address this issue.

The finding that the level of RhoA binding to membranes induced by triggering nucleotide exchange on RhoA−RhoGDIα was marginal relative to Cdc42 suggests that RhoA may bind either with higher affinity to RhoGDI or with lower affinity to the EYPC/DAG membranes compared to Cdc42. The possibility that the apparent decrease in the extent of dissociation of the RhoA−RhoGDIα complex and/or membrane association of RhoA upon nucleotide exchange might be due to differences in nucleotide exchange kinetics is unlikely since these have been reported previously to be similar for Cdc42 and RhoA (*76*). By contrast to the lack of binding of RhoA to EYPC/DAG/POPS membranes reported here, a recent study showed recently that nucleotide exchange

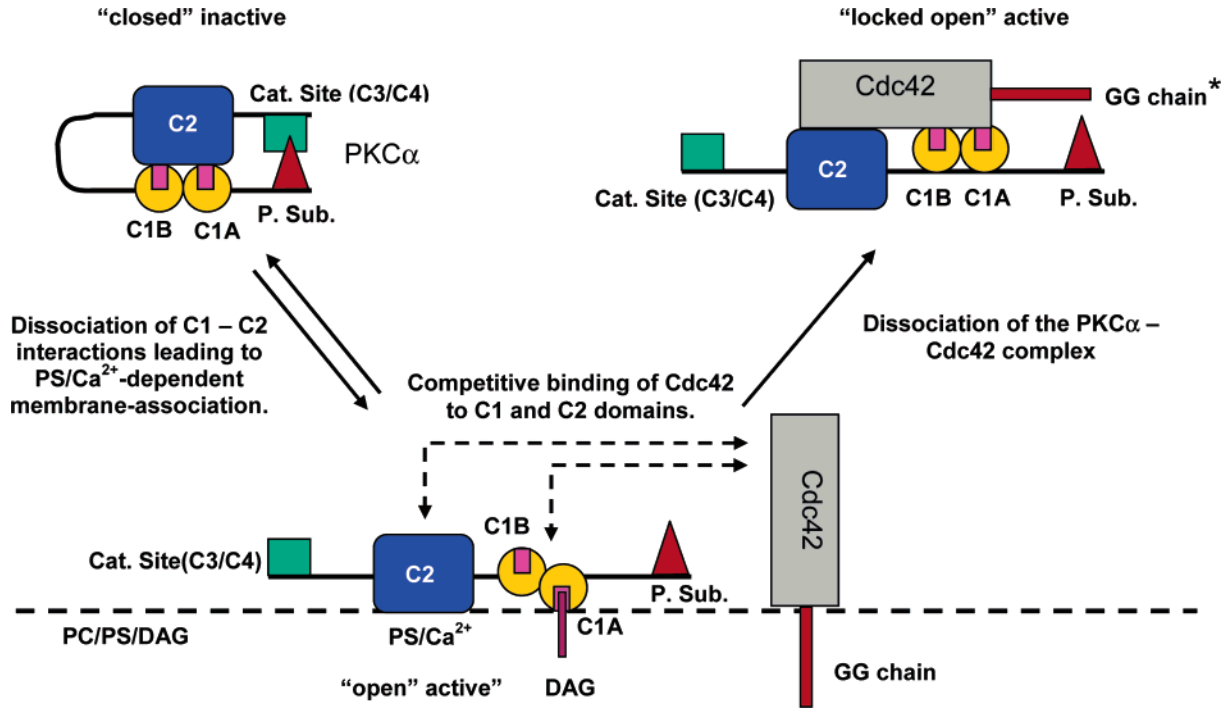

FIGURE 8: Model for PKCα membrane association governed by competitive protein−protein and protein−lipid interactions. The membrane association of PKCα results from the dissociation of intramolecular C1 and C2 domain interactions due to binding of DAG and PS/Ca^{2+} to these domains at the membrane surface (*11*, *67*, *68*, *77*−*85*). This corresponds to a conformational shift from a closed inactive to an open active form. Membrane-bound Cdc42 competes for PS/Ca^{2+} interactions with the C2 domain and, based on the results of a previous study, also interacts with the C1 domains (*39*), leading to a net decrease in membrane-binding affinity and dissociation of the PKCα−Cdc42 complex from the membrane. Binding of Cdc42 to the C1 and C2 domains competes for C1−C2 domain interactions and locks the PKCα molecule in an open active form that no longer requires DAG or Ca^{2+} for its stabilization. The specific activity of Cdc42-bound PKCα is reduced compared to the membrane-associated form. *****Note that this model also requires that the geranylgeranyl (GG) chain of Cdc42 be incorporated into an, as yet, unknown region of the PKCα molecule.

on RhoA was sufficient to induce its release from RhoGDI and for association with liposomes composed of purified lipids derived from *Escherichia coli* membranes (*73*). This apparent difference in results may arise from the presence of lipid factors in *E. coli* membranes, not present in those used here, that promote RhoA−RhoGDIα complex dissociation and/or RhoA membrane association. Further studies are required to address the interesting question whether Rho GTPase binding to membranes can be modulated by changes in membrane lipid composition.

Membrane-Bound Cdc42 Reduces PKCα Membrane Binding Affinity by Competing for PS and Ca^{2+} Interactions. The observation that the membrane association of PKCα was inhibited by membrane-bound Cdc42 supports the contention that these proteins engage in a specific protein−protein interaction at the membrane surface. Evidence for this was provided by the finding that the inhibitory effect of membrane-bound Cdc42 on membrane association was confined to PKCα, which is similar to the isozyme specificity reported previously for the direct protein−protein interaction with Rho GTPases determined in the absence of membranes (*44*). Further evidence for a specific interaction between PKCα and Cdc42 at the membrane surface was provided by the finding that the extent of the inhibitory effect of Cdc42 on PKCα membrane association was dependent on both the concentration of PKCα (Figure 7B, inset) and membrane-bound Cdc42 (Figure 3A, inset). Also, the observation that an excess of Mg^{2+} failed to replace Ca^{2+} in enhancing the PKCα-mediated Cdc42 extraction from membranes (results not shown) is consistent with the established specificity of the C2 domain of PKCα for Ca^{2+} binding and again supports a specific interaction between the two proteins.

The finding that the presence of Cdc42 at the surface of membranes resulted in a shift in the PKCα binding isotherm to the right is consistent with a reduction in membrane-binding affinity and suggests competitive binding of PKCα to membranes and to Cdc42 (Figure 2A). On the basis of the rightward shift in both the POPS- and Ca^{2+}-concentration curves for membrane association (Figures 3 and 4), it appears that this reduced binding affinity results from competition between Cdc42 and PS/Ca^{2+} interactions with PKCα. Since the Ca^{2+} binding loops of the C2 domain of PKCα contain the site(s) of interaction of PS and Ca^{2+} (see, e.g., ref *67*), this suggests that Cdc42, and potentially other Rho GTPases including RhoA, may compete with PS/Ca^{2+} for binding to overlapping sites within this region. However, the finding that the presence of Cdc42 at the surface of EYPC/DAG membranes without POPS also resulted in a reduction of the extent of PKCα membrane association suggests that Cdc42 may compete for regions on the PKC molecule in addition to the C2 domain that also stabilize the membrane interaction. Consistent with these findings, it was shown recently that the PS/Ca^{2+}-binding C2 domain as well as the DAG-binding C1 domains of PKCα contains sites that participate in the direct protein−protein interaction with RhoA in the absence of membranes (*39*). This would provide a plausible mechanism for the apparent reduction in membrane-binding affinity since a displacement of PS/Ca^{2+} binding to the C2 domain and DAG binding to the C1 domain by Cdc42 would weaken the PKCα−membrane interaction.

Membrane-Bound Cdc42 Reduces PKCα Membrane-Associated Activity. In addition to decreasing membrane-binding affinity, the interaction of Cdc42 with PKCα also appears to result in a decrease in PKCα activity relative to that obtained for the membrane-associated enzyme in the absence of the GTPase (Figure 4). The observation that the level of activity obtained in the presence of EYPC/DAG membranes and Cdc42 was close to that measured for PKCα in complex with Cdc42 in the absence of membranes (Figure 4A, inset, and ref *44*) is again consistent with a reduction in the membrane-binding affinity of PKCα. Furthermore, the finding that the presence of membrane-bound Cdc42 shifted the PS- and Ca^{2+}-concentration response curves for PKCα activation to the right without affecting the maximal level of activity achieved (Figure 4) again suggests competition between Cdc42 and PS/Ca^{2+} for binding to the C2 domain of PKC.

The PKCα−Cdc42 Complex Physically Dissociates from Membranes. The results of this study are consistent with a model in which PKCα interacts with Cdc42 at the membrane surface to form a complex that possesses a reduced membrane-binding affinity, due to competition between Cdc42 and PS/Ca^{2+} interactions (Figure 8). The finding that the presence of Cdc42 resulted in a decrease in the level of PKCα binding at equilibrium to membranes in FC1 supports a "noncompetitive" type of mechanism in which the PKCα−Cdc42 complex formed by direct interaction between the proteins is physically removed from this flow cell under the continuous flow conditions present in the Biacore system. Evidence supporting this was provided by the observation that PKCα injection over membranes containing 6×His-tagged Cdc42 in FC1 resulted in specific binding of the PKCα−Cdc42 complex to a DOGS-NTA/Ni^{2+} surface in FC2 (Figure 5). Also, the observation that the addition of PKCα resulted in a dequenching of MANT-GMP-PNP-loaded Cdc42 fluorescence due to FRET with membrane-associated HAF (Figure 6) provides further evidence supporting the membrane dissociation of the PKCα−Cdc42 complex.

The observation that the level of binding of the PKCα−Cdc42 complex to the DOGS-NTA/Ni^{2+} surface in FC2 upon injection of PKCα over the EYPC/DAG/POPS membrane was *reduced* compared to that obtained for injection over membranes lacking POPS is again consistent with competition between Cdc42 and PS/Ca^{2+} interactions with PKCα. This is also supported by the finding that the dequenching effect of PKCα addition on MANT fluorescence due to FRET with membrane-associated HAF was reduced in the presence of POPS (Figure 7). Moreover, the finding that the addition of Ca^{2+} enhanced the dequenching effect of PKCα addition (Figure 6B) again suggests that the Ca^{2+}/PS-binding C2 domain might contribute to the interaction between PKCα and Cdc42 at the membrane surface. In connection with this, we have shown previously that Ca^{2+} is absolutely required for the formation of the direct protein−protein interaction between PKCα and Rho GTPases in the absence of membranes (*44*). Since PKCα also binds to PS in a Ca^{2+}-dependent manner (*5*, *12*), the extent by which Cdc42 is extracted from PS-containing membranes by PKCα is predicted to be a function of the relative Ca^{2+}-binding affinities of the PS-bound and Cdc42-bound enzyme.

The observation that the interaction of PKCα with membrane-bound Cdc42 resulted in the dissociation of the complex from the membrane suggests that PKCα may act in an analogous manner to RhoGDIα which also extracts Rho GTPases from membranes by virtue of a direct protein−protein interaction (*16*). However, since the interactions of RhoGDIα and PKCα with the membrane and with Cdc42 differ, it is likely that divergent mechanisms are involved in the extraction of Cdc42 from membranes by each protein. For example, contrasting with RhoGDIα, PKCα interacts with membranes in a Ca^{2+}- and PS-dependent manner. The apparent difference in the rates of extraction induced by RhoGDIα compared to PKCα may therefore reflect divergent affinities of each protein for binding to membranes and to Cdc42 (see Figure 7A). Experiments designed to investigate the details of the mechanism by which PKCα extracts membrane-bound Cdc42 are currently underway in the laboratory.

The interaction of Rho GTPases with membranes involves the insertion of a hydrophobic geranylgeranyl chain into the membrane interior, which is otherwise occluded by interaction with a hydrophobic pocket within the globular C-terminal fold of RhoGDIα (*52*). Thus, the observed dissociation of Cdc42 from the membrane in complex with PKCα implies that a hydrophobic region capable of shielding the geranylgeranyl chain from the aqueous environment may also exist within the PKCα molecule. Furthermore, our previous study showed that the presence of a phorbol ester or a soluble DAG is required for the optimal formation of the membrane-independent protein−protein interaction between PKCα and Rho GTPases (*44*, *45*). Since the diglyceride used in the present study is hydrophobic and would therefore be expected to be partitioned into the membrane, the question arises how the stability of the PKCα−Cdc42 complex is maintained in the absence of DAG as it dissociates from the membrane. It is hypothesized that the binding of Cdc42 to PKCα irreversibly *locks* the protein conformation in an active conformational form that no longer requires DAG or Ca^{2+} for stabilization. In this regard, it has been proposed that the activation of PKCα results from a conformational shift from a "closed" inactive to an "open" active form, which is controlled by the dissociation of intramolecular C1 and C2 domain interactions that occurs upon binding of DAG and PS/Ca^{2+} to these domains at the membrane surface (*11*, *67*, *68*, *77*−*85*). Thus, on the basis of the present data and the results of a previous study (*39*), which indicated an interaction of Cdc42 with the C2 domain, we hypothesize that Cdc42 might also compete for these intramolecular C1−C2 domain interactions, leading to a shift of the conformational equilibrium from the closed inactive toward a "locked open" active state (see Figure 7). Consistent with this, we have shown previously that the direct protein−protein interaction between PKCα and Rho GTPases, including Cdc42, results in kinase activation (*44*).

CONCLUSION

The finding that the net binding affinity of PKCα for membranes containing Rho GTPases is a product of the affinities of competing protein−protein and protein−lipid interactions provides a novel mechanism for the regulation of membrane-associated PKCα activity. In particular, since we have previously shown that the formation of a direct protein−protein interaction with Rho GTPases is a specific property of PKC (*44*), the interaction with membrane-bound

Cdc42, which is shown here to share this isozyme specificity, may serve to target this particular isozyme to specific regions of the plasma membrane and therefore localize it with specific downstream targets. In this regard, the function of the interaction of PKCα with Cdc42 may be analogous to those formed with a growing family of PKC binding proteins that mediate the recruitment of individual isozymes to specific signaling complexes involved in discrete signaling cascades (*86*−*88*). The PKCα−Cdc42 interaction at the membrane surface and the ensuing decrease in membrane-binding affinity should, however, be viewed in the context of an extended network of protein−protein and protein−lipid interactions involving these proteins, and caution should be engendered in drawing the conclusion that an *identical* interaction occurs in the cellular environment. Nevertheless, the observation that the interaction of PKCα with Cdc42 at the membrane surface results in the dissociation of the PKCα−Cdc42 complex raises the intriguing possibility that PKCα might act in an analogous manner to RhoGDI in the termination of Cdc42 signal by disabling interactions with downstream effectors.

ACKNOWLEDGMENT

We thank Dr. Christopher D. Stubbs for formative contributions to this work, Dr. Frank J. Taddeo for early contributions to the preparation of recombinant PKCα, Dr. Richard A. Cerione (Cornell University, New York) for providing the Cdc42 baculovirus, and Dr. William S. Blaner (Columbia University, New York) for providing HSC-T6 cells.

REFERENCES

1. Vaughan, P. F., Walker, J. H., and Peers, C. (1998) *Mol. Neurobiol. 18*, 125−155.
2. Mellor, H., and Parker, P. J. (1998) *Biochem. J. 332*, 281−292.
3. Nishizuka, Y. (1995) *FASEB J. 9*, 484−496.
4. Jaken, S. (1996) *Curr. Opin. Cell Biol. 8*, 168−173.
5. Newton, A. C. (1997) *Curr. Opin. Cell Biol. 9*, 161−167.
6. Dempsey, E. C., Newton, A. C., Mochly-Rosen, D., Fields, A. P., Reyland, M. E., Insel, P. A., and Messing, R. O. (2000) *Am. J. Physiol. 279*, L429−L438.
7. Parker, P. J., and Murray-Rust, J. (2004) *J. Cell Sci. 117*, 131−132.
8. Koivunen, J., Aaltonen, V., and Peltonen, J. (2006) *Cancer Lett. 235*, 1−10.
9. Newton, A. C. (1995) *J. Biol. Chem. 270*, 28495−28498.
10. Hurley, J. H., Newton, A. C., Parker, P. J., Blumberg, P. M., and Nishizuka, Y. (1997) *Protein Sci. 6*, 477−480.
11. Cho, W. (2001) *J. Biol. Chem. 276*, 32407−32410.
12. Newton, A. C. (1995) *Curr. Biol. 5*, 973−976.
13. House, C., and Kemp, B. E. (1987) *Science 238*, 1726−1728.
14. Makowske, M., and Rosen, O. M. (1989) *J. Biol. Chem. 264*, 16155−16159.
15. Orr, J. W., Keranen, L. M., and Newton, A. C. (1992) *J. Biol. Chem. 267*, 15263−15266.
16. Takai, Y., Sasaki, T., and Matozaki, T. (2001) *Physiol. Rev. 81*, 153−208.
17. Matozaki, T., Nakanishi, H., and Takai, Y. (2000) *Cell Signalling 12*, 515−524.
18. Zohn, I. M., Campbell, S. L., Khosravi-Far, R., Rossman, K. L., and Der, C. J. (1998) *Oncogene 17*, 1415−1438.
19. Ridley, A. J. (1999) *Prog. Mol. Subcell. Biol. 22*, 1−22.
20. Wennerberg, K., and Der, C. J. (2004) *J. Cell Sci. 117*, 1301−1312.
21. Dransart, E., Olofsson, B., and Cherfils, J. (2005) *Traffic 6*, 957−966.
22. Exton, J. H. (1998) *Biochim. Biophys. Acta 1436*, 105−115.
23. Bae, C. D., Min, D. S., Fleming, I. N., and Exton, J. H. (1998) *J. Biol. Chem. 273*, 11596−11604.
24. Park, S. K., Min, D. S., and Exton, J. H. (1998) *Biochem. Biophys. Res. Commun. 244*, 364−367.
25. Seifert, J. P., Snyder, J. T., Sondek, J., and Harden, T. K. (2006) *Methods Enzymol. 406*, 260−271.
26. Thodeti, C. K., Massoumi, R., Bindslev, L., and Sjolander, A. (2002) *Biochem. J. 365*, 157−163.
27. Watanabe, G., Saito, Y., Madaule, P., Ishizaki, T., Fujisawa, K., Morii, N., Mukai, H., Ono, Y., Kakizuka, A., and Narumiya, S. (1996) *Science 271*, 645−648.
28. Houssa, B., de Widt, J., Kranenburg, O., Moolenaar, W. H., and van Blitterswijk, W. J. (1999) *J. Biol. Chem. 274*, 6820−6822.
29. Amano, M., Mukai, H., Ono, Y., Chihara, K., Matsui, T., Hamajima, Y., Okawa, K., Iwamatsu, A., and Kaibuchi, K. (1996) *Science 271*, 648−650.
30. Flynn, P., Mellor, H., Palmer, R., Panayotou, G., and Parker, P. J. (1998) *J. Biol. Chem. 273*, 2698−2705.
31. Vincent, S., and Settleman, J. (1997) *Mol. Cell. Biol. 17*, 2247−2256.
32. Van Aelst, L., and D'Souza-Schorey, C. (1997) *Genes Dev. 11*, 2295−2322.
33. Aspenstrom, P. (1999) *Curr. Opin. Cell Biol. 11*, 95−102.
34. Coghlan, M. P., Chou, M. M., and Carpenter, C. L. (2000) *Mol. Cell. Biol. 20*, 2880−2889.
35. Hippenstiel, S., Kratz, T., Krull, M., Seybold, J., von Eichel-Streiber, C., and Suttorp, N. (1998) *Biochem. Biophys. Res. Commun. 245*, 830−834.
36. Chang, J. H., Pratt, J. C., Sawasdikosol, S., Kapeller, R., and Burakoff, S. J. (1998) *Mol. Cell. Biol. 18*, 4986−4993.
37. Nozu, F., Tsunoda, Y., Ibitayo, A. I., Bitar, K. N., and Owyang, C. (1999) *Am. J. Physiol. 276*, G915−G923.
38. Patil, S. B., and Bitar, K. N. (2006) *Am. J. Physiol. 290*, G83−G95.
39. Pang, H., and Bitar, K. N. (2005) *Am. J. Physiol. 289*, C982−C993.
40. Patil, S. B., Pawar, M. D., and Bitar, K. N. (2004) *Am. J. Physiol. 286*, G635−G644.
41. Bitar, K. N., Ibitayo, A., and Patil, S. B. (2002) *J. Appl. Physiol. 92*, 41−49.
42. Kamada, Y., Qadota, H., Python, C. P., Anraku, Y., Ohya, Y., and Levin, D. E. (1996) *J. Biol. Chem. 271*, 9193−9196.
43. Nonaka, H., Tanaka, K., Hirano, H., Fujiwara, T., Kohno, H., Umikawa, M., Mino, A., and Takai, Y. (1995) *EMBO J. 14*, 5931−5938.
44. Slater, S. J., Seiz, J. L., Stagliano, B. A., and Stubbs, C. D. (2001) *Biochemistry 40*, 4437−4445.
45. Slater, S. J., Cook, A. C., Seiz, J. L., Malinowski, S. A., Stagliano, B. A., and Stubbs, C. D. (2003) *Biochemistry 42*, 12105−12114.
46. Patton, C., Thompson, S., and Epel, D. (2004) *Cell Calcium 35*, 427−431.
47. Stabel, S., Schaap, D., and Parker, P. J. (1991) *Methods Enzymol. 200*, 670−673.
48. Taddeo, F. J. (1998) Cloning, expression and purification of protein kinase C: A comparative study of the modes of activation of protein kinase C, Ph.D., Thomas Jefferson University, Philadelphia, PA.
49. Slater, S. J., Kelly, M. B., Taddeo, F. J., Rubin, E., and Stubbs, C. D. (1994) *J. Biol. Chem. 269*, 17160−17165.
50. Slater, S. J., Taddeo, F. J., Mazurek, A., Stagliano, B. A., Milano, S. K., Kelly, M. B., Ho, C., and Stubbs, C. D. (1998) *J. Biol. Chem. 273*, 23160−23168.
51. Cerione, R. A., Leonard, D., and Zheng, Y. (1995) *Methods Enzymol. 256*, 11−15.
52. Hoffman, G. R., Nassar, N., and Cerione, R. A. (2000) *Cell 100*, 345−356.
53. Longenecker, K., Read, P., Derewenda, U., Dauter, Z., Liu, X., Garrard, S., Walker, L., Somlyo, A. V., Nakamoto, R. K., Somlyo, A. P., and Derewenda, Z. S. (1999) *Acta Crystallogr., Sect. D: Biol. Crystallogr. 55* (Part 9), 1503−1515.
54. Kato, M., Iwamoto, H., Higashi, N., Sugimoto, R., Uchimura, K., Tada, S., Sakai, H., Nakamuta, M., and Nawata, H. (1999) *J. Hepatol. 31*, 91−99.
55. Vogel, S., Piantedosi, R., Frank, J., Lalazar, A., Rockey, D. C., Friedman, S. L., and Blaner, W. S. (2000) *J. Lipid Res. 41*, 882−893.
56. MacDonald, R. C., MacDonald, R. I., Menco, B. P., Takeshita, K., Subbarao, N. K., and Hu, L. R. (1991) *Biochim. Biophys. Acta 1061*, 297−303.

57. Erb, E.-M., Chen, X., Allen, S., Roberts, C. J., Tendler, S. J. B., Davies, M. C., and Forsen, S. (2000) *Anal. Biochem. 280*, 29−35.
58. Anderluh, G., Besenicar, M., Kladnik, A., Lakey, J. H., and Macek, P. (2005) *Anal. Biochem. 344*, 43−52.
59. Slater, S. J., Milano, S. K., Stagliano, B. A., Gergich, K. J., Ho, C., Mazurek, A., Taddeo, F. J., Kelly, M. B., Yeager, M. D., and Stubbs, C. D. (1999) *Biochemistry 38*, 3804−3815.
60. Dietrich, C., Boscheinen, O., Scharf, K. D., Schmitt, L., and Tampe, R. (1996) *Biochemistry 35*, 1100−1105.
61. Nomanbhoy, T. K., and Cerione, R. (1996) *J. Biol. Chem. 271*, 10004−10009.
62. Nomanbhoy, T. K., Erickson, J. W., and Cerione, R. A. (1999) *Biochemistry 38*, 1744−1750.
63. Robbe, K., Otto-Bruc, A., Chardin, P., and Antonny, B. (2003) *J. Biol. Chem. 278*, 4756−4762.
64. Mosior, M., and Newton, A. C. (1998) *Biochemistry 37*, 17271−17279.
65. Mosior, M., and Epand, R. M. (1996) *Proc. Natl. Acad. Sci. U.S.A. 93*, 1907−1912.
66. Slater, S. J., Kelly, M. B., Taddeo, F. J., Rubin, E., and Stubbs, C. D. (1994) *J. Biol. Chem. 269*, 17160−17165.
67. Stahelin, R. V., Wang, J., Blatner, N. R., Rafter, J. D., Murray, D., and Cho, W. (2005) *J. Biol. Chem. 280*, 36452−36463.
68. Slater, S. J., Seiz, J. L., Cook, A. C., Buzas, C. J., Malinowski, S. A., Kershner, J. L., Stagliano, B. A., and Stubbs, C. D. (2002) *J. Biol. Chem. 277*, 15277−15285.
69. Huang, S. M., Leventhal, P. S., Wiepz, G. J., and Bertics, P. J. (1999) *Biochemistry 38*, 12020−12027.
70. Sando, J. J., Chertihin, O. I., Owens, J. M., and Kretsinger, R. H. (1998) *J. Biol. Chem. 273*, 34022−34027.
71. Keranen, L. M., and Newton, A. C. (1997) *J. Biol. Chem. 272*, 25959−25967.
72. Newton, A. C., and Koshland, D. E., Jr. (1989) *J. Biol. Chem. 264*, 14909−14915.
73. Read, P. W., Liu, X., Longenecker, K., Dipierro, C. G., Walker, L. A., Somlyo, A. V., Somlyo, A. P., and Nakamoto, R. K. (2000) *Protein Sci. 9*, 376−386.
74. Del Pozo, M. A., Kiosses, W. B., Alderson, N. B., Meller, N., Hahn, K. M., and Schwartz, M. A. (2002) *Nat. Cell Biol. 4*, 232−239.
75. Bokoch, G. M., Bohl, B. P., and Chuang, T. H. (1994) *J. Biol. Chem. 269*, 31674−31679.
76. Zhang, B., Zhang, Y., Wang, Z., and Zheng, Y. (2000) *J. Biol. Chem. 275*, 25299−25307.
77. Ananthanarayanan, B., Stahelin, R. V., Digman, M. A., and Cho, W. (2003) *J. Biol. Chem. 278*, 46886−46894.
78. Bittova, L., Stahelin, R. V., and Cho, W. (2000) *J. Biol. Chem. 11*, 11.
79. Medkova, M., and Cho, W. (1999) *J. Biol. Chem. 274*, 19852−19861.
80. Conesa-Zamora, P., Gomez-Fernandez, J. C., and Corbalan-Garcia, S. (2000) *Biochim. Biophys. Acta 1487*, 246−254.
81. Oancea, E., Teruel, M. N., Quest, A. F., and Meyer, T. (1998) *J. Cell Biol. 140*, 485−498.
82. Oancea, E., and Meyer, T. (1998) *Cell 95*, 307−318.
83. Kirwan, A. F., Bibby, A. C., Mvilongo, T., Riedel, H., Burke, T., Millis, S. Z., and Parissenti, A. M. (2003) *Biochem. J. 373*, 571−581.
84. Guo, B., Reed, K., and Parissenti, A. M. (2006) *J. Mol. Biol. 357*, 820−832.
85. Rodriguez-Alfaro, J. A., Gomez-Fernandez, J. C., and Corbalan-Garcia, S. (2004) *J. Mol. Biol. 335*, 1117−1129.
86. Schechtman, D., and Mochly-Rosen, D. (2001) *Oncogene 20*, 6339−6347.
87. Mochly-Rosen, D., and Gordon, A. S. (1998) *FASEB J. 12*, 35−42.
88. Newton, A. C. (1996) *Curr. Biol. 6*, 806−809.

BI0612420